

# Microwave Spectra of Pyrolytically Produced $\text{CH}_3\text{NHCN}$ and $\text{CD}_3\text{NHCN}$ , *N*-Cyanomethylamine

BØRGE BAK and HENRIK SVANHOLT

Chemical Laboratory V, The H. C. Ørsted Institute, University of Copenhagen, DK-2100 Copenhagen, Denmark

Dimethylcyanamide,  $(\text{CH}_3)_2\text{NCN}$ , pyrolyzes (900 °C, 0.01 Torr) to  $\text{CH}_3\text{NHCN}$  as seen by its microwave spectrum (18.6–40.0 GHz). The spectral assignment was greatly facilitated by analysis of the microwave spectrum of  $\text{CD}_3\text{NHCN}$  produced by pyrolysis of  $(\text{CD}_3)_2\text{NCN}$ . The resulting structural information on  $\text{CH}_3\text{NHCN}$  is strictly limited by the use of assumed geometric parameters from other molecules ( $\text{CH}_3\text{NHCl}$ ,  $\text{CH}_3\text{C}\equiv\text{CH}$  and  $\text{CH}_3\text{N}_3$ ). An estimated barrier to internal torsion is  $260\text{ cm}^{-1}$  with a corresponding torsional frequency of *ca.*  $105\text{ cm}^{-1}$ . Approximate values of the  $\mu_a$  and  $\mu_b$ , electric dipole moment components are 4.72 and 1.30 Debye, respectively.

During an extended microwave (mw) spectroscopic analysis of products of pyrolysis of  $(\text{CH}_3)_2\text{NCN}$  (1000 °C,  $p \sim 0.01$  Torr) where a main and easily identified product is  $\text{CH}_2=\text{NCN}$  or  $(\text{HCN})_2$ ,<sup>1</sup> a weaker spectrum was subsequently observed (900 °C,  $p \sim 0.01$  Torr; spec. H). In addition,  $(\text{CD}_3)_2\text{NCN}$  was pyrolyzed giving rise to another "weak" spectrum, spec. D. Comparison of spec.'s H and D showed features familiar from mw spectra of molecules with an internally rotating  $\text{CH}_3$  group and with NH inversion. A reasonable guess at the origin of spec.'s H and D is, therefore,  $\text{CH}_3\text{NHCN}$  (I) and  $\text{CD}_3\text{NHCN}$  (II) since primarily formed  $\text{CD}_3\text{NDCN}$  (III) will exchange mobile nitrogen-bound D by H due to the presence of  $\text{H}_2\text{O}$  in the mw cell. The mw spectrum of II is of greater interest to the present problem because the spectral effects of inversion are conserved whereas the effects of  $\text{CH}_3$  internal rotation are largely annulled.

A more tangible verification of the formulae of I and II was obtained by calculation of rotational

constants (*A, B, C*) of rigid models of I and II formed from parameters for related molecules (*vide infra*). These models predicted near-prolate symmetric top mw spectra close to their actual positions, without, of course, accounting for the observed spectral multiplicity due to  $\text{CH}_3$  torsion ('a, e splitting') and NH inversion.

Molecules with both effects have been studied earlier [ $(\text{CH}_3)_2\text{NH}$ ;<sup>2</sup>  $\text{CH}_3\text{NHCl}$ ].<sup>3</sup> Following the usual  $\pm$  notation for inversion, 8 spectra are expected:

Spec. H: I(a, +); I(e, +); I(a, -); I(e, -).

Spec. D: II(a, +); II(e, +); II(a, -); II(e, -).

Corresponding frequency ( $\nu$ ) differences are expected to obey

$$\begin{aligned} \nu\text{I}(a, +) - \nu\text{I}(a, -) &\sim \nu\text{II}(a, +) - \nu\text{II}(a, -) \\ \nu\text{I}(a, +) - \nu\text{I}(e, +) &\sim \nu\text{I}(a, -) - \nu\text{I}(e, -) \\ \nu\text{I}(a, +) - \nu\text{I}(e, +) &> \nu\text{II}(a, +) - \nu\text{II}(e, +) \\ \nu\text{I}(a, -) - \nu\text{I}(e, -) &> \nu\text{II}(a, -) - \nu\text{II}(e, -) \end{aligned}$$

in the absence of vibrational interactions. The spectra I(a, +), I(a, -), II(a, +) and II(a, -) are expected to be reproducible by conventional rigid rotor models  $M_{\text{H}}(+)$ ,  $M_{\text{H}}(-)$ ,  $M_{\text{D}}(+)$  and  $M_{\text{D}}(-)$  whereas this is not possible for 'e' spectra. As a consequence of the subsequent analysis (Tables 1-4) we have restricted ourselves to deriving  $M_{\text{H}}(+)$  and  $M_{\text{D}}(+)$ .

## EXPERIMENTAL

Our equipment for performing pyrolysis and analysis by mw technique has been described else-

where.<sup>4</sup>  $\text{CH}_3\text{NHCN}$ , here prepared conveniently by pyrolysis, has been produced earlier at  $-10^\circ\text{C}$  from  $\text{CH}_3\text{NH}_2$  and  $\text{BrCN}$  (m.p.  $-40^\circ\text{C}$  to  $-50^\circ\text{C}$ ; polymerization at  $+50^\circ\text{C}$ ).<sup>5</sup> Following Ref. 5 strictly in a single experiment we found that polymerization was dominant even at the final removal of the solvent (dry ether) at low temperature ( $\sim -20^\circ\text{C}$ ). A small yield was, however, collected and its mw spectrum recorded at room temperature

(no pyrolysis). Very strong absorption, identical with spec. H, was observed.

When pyrolyzing ( $1000^\circ\text{C}$ ,  $p \sim 0.02$  Torr) vapors from the synthetic product no lines from  $\text{CH}_2=\text{NCN}$  were found.  $(\text{CH}_3)_2\text{NCN}$  may, therefore, pyrolyze in two ways:

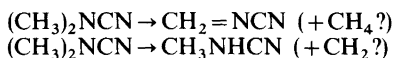


Table 1. Observed  $2_{02}-3_{03}$  transitions (MHz) of approximately equal intensity in  $\text{CH}_3\text{NHCN}$  (I) and  $\text{CD}_3\text{NHCN}$  (II) in order of increasing frequency.  $i$  = inversion effect;  $a,e$  = torsional effect.

					$\langle i \rangle$	$\langle a,e \rangle$
I	28417.73	28425.05	28463.76	28471.54		
Average		28421.39		28467.65	46.26	
$a,e$		7.32		7.78		7.55
II	25348.10	25349.54	25384.63	25387.23		
Average		25348.82		25385.93	37.11	
$a,e$		1.44		2.60		2.02

Table 2. Observed and assigned rotational ( $a,+$ ) transitions<sup>a</sup> (18.6–40.0 GHz) for  $\text{CH}_3\text{NHCN}$  (I) and  $\text{CD}_3\text{NHCN}$  (II).

	I( $a,+$ )			II( $a,+$ )		
	Obs.	Obs. – calc. Fit incl. $\Delta_J, \Delta_{JK}$	Rigid rotor fit	Obs.	Obs. – calc. Fit incl. $\Delta_J, \Delta_{JK}$	Rigid rotor fit
$1_{11}-2_{12}$	18492.5 <sup>b</sup>	0.04				
$1_{01}-2_{02}$	18959.17	0.10	0.25			
$1_{10}-2_{11}$	19435.8 <sup>b</sup>	0.67				
$2_{12}-3_{13}$	27735.21	0.09	0.11	24781.50	0.08	1.49
$2_{02}-3_{03}$	28425.05	0.03	0.11	25349.54	-0.04	0.95
$2_{11}-3_{12}$	29151.19	0.09	0.11	25948.62	-0.04	1.37
$2_{21}-3_{22}$	28447.0	0.25	0.55	25367 <sup>c</sup>	0.60	
$2_{20}-3_{21}$	28467.5	-0.57	-0.46	25386 <sup>c</sup>	0.66	
$3_{13}-4_{14}$	36973.68	0.13	-0.27	33036.13	0.01	1.25
$3_{03}-4_{04}$	37874.66	-0.06	-0.19	33777.07	0.03	-0.27
$3_{12}-4_{13}$	38861.47	0.12	-0.27	34592.39	0.11	1.34
$3_{22}-4_{23}$	37923.8	-0.58	-0.62	33817.6	-0.25	-0.82
$3_{21}-4_{22}$	37977.8	0.17	-0.37	33865.2	0.00	2.24
$3_{31}-4_{32}$	37940.0	0.24	0.75	33827.5	0.15	-3.20
$3_{30}-4_{31}$	37940.0	0.01	0.52	33827.5	-0.06	-3.40
rms		0.33	0.46		0.15	2.27

<sup>a</sup> Peaks of unresolved quadrupole coupling patterns. <sup>b</sup> Diffuse quadrupole coupling pattern. Not included in fits. <sup>c</sup> Tentative. Not included in fits.

but our experiments do not exclude other mechanisms. The applied  $(\text{CD}_3)_2\text{NCN}$  was prepared as referred elsewhere.<sup>6</sup>

#### ASSIGNMENT. DIPOLE MOMENT

Close to the centers of observed 1→2, 2→3 and 3→4 rotational transitions of I and II their mw

spectra at 400 V/cm are dominated by quartets as exemplified in Table 1. In agreement with the isotope shift rules for  $\text{CH}_3\text{NHCN} \rightarrow \text{CD}_3\text{NHCN}$  sketched above transitions in columns 2 and 3 tentatively were assigned to I(a,+), I(e,+), II(a,+) and II(e,+) while transitions in columns 4 and 5 have the inversion character -1. The final assign-

Table 3. Observed and assigned rotational (a,-) transitions<sup>a</sup> (18.6–40.0 GHz) for  $\text{CH}_3\text{NHCN}$  (I) and  $\text{CD}_3\text{NHCN}$  (II).

	I(a,-)			II(a,-)		
	Obs.	Obs. - calc. Fit incl. $\Delta_J, \Delta_{JK}$	Rigid rotor fit	Obs.	Obs. - calc. Fit incl. $\Delta_J, \Delta_{JK}$	Rigid rotor fit
$1_{11} - 2_{12}$	18522.0 <sup>b</sup>	1.00				
$1_{01} - 2_{02}$	18984.93	0.10	-1.75			
$1_{10} - 2_{11}$	19460.5 <sup>b</sup>	-0.4				
$2_{12} - 3_{13}$	27778.34	0.25	-1.95	24819.29	0.01	-2.95
$2_{02} - 3_{03}$	28463.76	0.06	-1.45	25384.63	0.05	-1.86
$2_{11} - 3_{12}$	29188.15	0.23	-1.98	25984.31	-0.07	-3.06
$2_{21} - 3_{22}$						
$2_{20} - 3_{21}$	28510.5	-0.68	-2.13			
$3_{13} - 4_{14}$	37031.17	-0.01	-2.41	33086.57	0.13	-3.53
$3_{03} - 4_{04}$	37926.22	-0.14	0.24	33823.84	0.11	0.48
$3_{12} - 4_{13}$	38910.77	0.00	-2.38	34639.93	0.19	-3.45
$3_{22} - 4_{23}$	37981.7	-0.12	1.09	33873.8	-0.83	0.43
$3_{21} - 4_{22}$	38036.0	0.15	-3.86	33921.5	0.08	-6.11
$3_{31} - 4_{32}$	38004.0	0.20	7.05	33897.5	0.25	9.18
$3_{30} - 4_{31}$	38004.0	-0.03	6.77	33897.5	0.04	8.90
rms		0.32	3.95		0.41	5.94

<sup>a</sup> Peaks of unresolved quadrupole coupling patterns. <sup>b</sup> Diffuse. Not included in fits.

Table 4. Rotational constants  $A, B, C$  (MHz) and centrifugal distortion constants  $\Delta_J$  and  $\Delta_{JK}$  (kHz) for  $\text{CH}_3\text{NHCN}(a,+)$ ,  $\text{CD}_3\text{NHCN}(a,+)$ ,  $\text{CH}_3\text{NHCN}(a,-)$  and  $\text{CD}_3\text{NHCN}(a,-)$  spectra as analyzed by ROTFIT.

	I(a,+)	II(a,+)	I(a,-)	II(a,-)
$A$	$36090 \pm 156$	$28190 \pm 64$	$35380 \pm 145$	$28390 \pm 178$
$B$	$4977.13 \pm 0.07$	$4422.69 \pm 0.04$	$4982.54 \pm 0.07$	$4428.16 \pm 0.11$
$C$	$4505.13 \pm 0.07$	$4033.59 \pm 0.04$	$4512.58 \pm 0.07$	$4039.78 \pm 0.11$
$\Delta_J$	$4.3 \pm 2.0$	$2.9 \pm 1.3$	$0.4 \pm 2.1$	$5.0 \pm 3.4$
$\Delta_{JK}$	$-17.4 \pm 5.3$	$89.1 \pm 2.5$	$-176.7 \pm 5.2$	$-242.7 \pm 6.7$
rms <sup>a</sup>	0.33	0.15	0.32	0.41
rms <sup>b</sup>	0.46	2.27	3.95	5.94

<sup>a</sup> Fit including  $\Delta_J$  and  $\Delta_{JK}$ . <sup>b</sup> Rigid rotor fit.

ments of I(a,+), II(a,+), I(a,-) and II(a,-) spectra are reported in Tables 2 and 3. A ROTFIT program<sup>7</sup> was used implying rotational constants  $A, B, C$  and centrifugal distortion constants  $\Delta_J$  and  $\Delta_{JK}$ . Rather large irregularities for  $\Delta_J$  and  $\Delta_{JK}$  were found (Table 4). For purpose of clarification a ROTFIT for  $\Delta_J = \Delta_{JK} = 0$  is included in Tables 2 and 3. As seen, this works well for CH<sub>3</sub>NHCN suggesting that perturbations not taken into account for the II(a,+), I(a,-) and II(a,-) spectra do occur. For I(a,-) and II(a,-) this may be due to their status as excited states. The  $[E(a,-) - E(a,+)]$  energy difference is not known to us because of failure to observe  $\mu_c$  transitions. For II(a,+) and II(a,-) it must be noted that CD<sub>3</sub>NHCN possesses normal vibrations of lower frequency than CH<sub>3</sub>NHCN. For

these reasons the association of a model M<sub>H</sub>(+) with the I(a,+) spectrum involves minimum errors. Larger errors are involved in M<sub>D</sub>(+) also presented (*vide infra*) (Table 5) agreeing with the fact (Table 6) that reasonably well predicted a,e splittings are obtained for the I(a,+), I(e,+) spectra only. The applied computer program SEM-4 ignores any interaction between CH<sub>3</sub> and CD<sub>3</sub> torsion and other modes including inversion.

Following the M = 1 component of the transitions  $2_{12} \rightarrow 3_{13}$  (300 V/cm),  $2_{11} \rightarrow 3_{12}$  (300 V/cm),  $3_{13} \rightarrow 4_{14}$  (800 V/cm) and  $3_{12} \rightarrow 4_{13}$  (800 V/cm) in the spectrum I(a,+) yielded dipole moment components  $\mu_a = 4.72$  Debye;  $\mu_b = 1.30$  Debye while a small  $\mu_c$  could not be fixed. The values of  $\mu_a$  and  $\mu_b$  are approximate. All assigned transitions are of  $\mu_a$  type.

Table 5. Model rotational constants (MHz) compared to experimental rotational constants of CH<sub>3</sub>NHCN and CD<sub>3</sub>NHCN. Model 2→3 transitions compared to observed transitions.

	CH <sub>3</sub> NHCN Obs.	Model M <sub>H</sub> (+)	CD <sub>3</sub> NHCN Obs.	Model M <sub>D</sub> (+)
A	36090	33547	28190	27148
B	4977.13	4977.13	4422.69	4422.69
C	4505.13	4505.13	4033.59	4033.59
$2_{12} - 3_{13}$	27735.21	27735.16	24781.50	24782.11
$2_{02} - 3_{03}$	28425.05	28423.57	25349.54	25349.03
$2_{11} - 3_{12}$	29151.19	29151.11	25948.62	25949.37
$2_{21} - 3_{22}$	28447.0	28446.76	25367	25368.84
$2_{20} - 3_{21}$	28467.5	28469.96	25387	25388.65
Angles <sup>a</sup>				
$\alpha$ (°)		179.92		177.88
$w$ (°)		112.90		112.50

<sup>a</sup> Fig. 1.

Table 6. Experimental I(e,+) and II(e,+) frequencies (MHz). Experimental and calculated differences I(a,+) - I(e,+) and II(a,+) - II(e,+). I(a,+) and II(a,+) frequencies in Table 2. I = CH<sub>3</sub>NHCN; II = CD<sub>3</sub>NHCN.

	I(e,+)	I(a,+) - I(e,+)		II(e,+)	II(a,+) - II(e,+)	
		Exp.	Calc.		Exp.	Calc.
$1_{01} - 2_{02}$	18954.28	4.89	6.36			
$2_{12} - 3_{13}$	27822.18	-86.97	-86.64	24782.63	-1.13	-1.16
$2_{02} - 3_{03}$	28417.73	7.32	6.76	25348.10	1.44	-0.34
$2_{11} - 3_{12}$	29051.35	99.84	93.96	25945.33	3.29	-0.79
$3_{13} - 4_{14}$	37012.0	-38.32	-40.85	33036.13	0.00	-1.51
$3_{03} - 4_{04}$	37865.15	9.51	4.12	33775.14	1.93	-2.05
$3_{12} - 4_{13}$	38805.8	55.67	39.47	34588.90	3.49	-4.54

## MOLECULAR MODELS

$M_H(+)$  and  $M_D(+)$  models corresponding to ROTFIT rotational constants (Table 4) have been worked out. With only two well-determined rotational constants per species,  $B$  and  $C$ , a number of assumptions has to be made. We have chosen to assume corresponding structural parameters from related  $\text{CH}_3\text{NHCl}$  (method I of Ref. 9). Referring to Fig. 1 we have further taken the  $\text{N1}-\text{C2}$  distance as  $1.400 \text{ \AA}$  ( $\sim 1.459 \text{ \AA}$  as in  $\text{CH}_3-\text{C}\equiv\text{CH}$  minus a carbon, nitrogen covalent radius difference of  $0.055 \text{ \AA}$ ) and the  $\text{C2}\equiv\text{N2}$  distance as  $1.160 \text{ \AA}$ . Then the angles  $\alpha$  and  $w$  were fitted to reproduce  $B$  and  $C$ . The result is reported in Table 5. Obviously,  $\alpha$  and  $w$  are practically independent of their molecular affiliation. Their dependence on the badly fixed rotational constant  $A$  is also slight as seen by the consistency between observed  $2_{i,j} \rightarrow 3_{i,j+1}$  transition frequencies and frequencies based on the rigid models. The models  $M_H(+)$  and  $M_D(+)$  were used for the calculations of 'a,e splittings' to follow.

TORSIONAL SPLITTINGS IN  $\text{CH}_3\text{NHCN}$  AND  $\text{CD}_3\text{NHCN}$ 

Unusually large Stark splittings at the band centres where intense spectra could be observed even at an electric field of  $1 \text{ V/cm}$ , together with our use of SEM-4 (imperfect for our purpose)

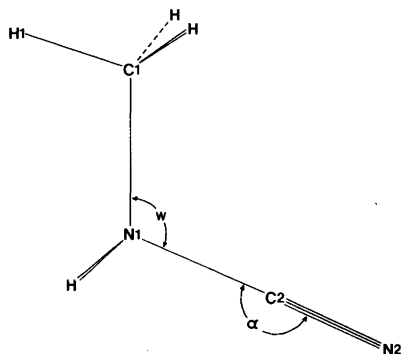


Fig. 1. Rigid model of  $\text{CH}_3\text{NHCN}$ . Atoms  $\text{H1}$ ,  $\text{C1}$ ,  $\text{N1}$ ,  $\text{C2}$  and  $\text{N2}$  in plane of paper. Calculated structural parameters  $\alpha$  ( $178-180^\circ$ ) and  $w$  ( $112.5-113^\circ$ ) based on assumed remaining angles and interatomic distances (see text). The resulting angles agree well with corresponding angles in  $\text{CH}_3\text{CH}_2\text{CN}$  in which ' $\alpha$ ' =  $178.73^\circ$  and ' $w$ ' =  $111.98^\circ$ .<sup>11</sup>

proved serious enough to prevent unambiguous assignment of about half of the 'e' transitions. Transitions, safely assigned by their Stark patterns and their relatively isolated location (except for the  $2_{02} \rightarrow 3_{03}$  and  $3_{03} \rightarrow 4_{04}$  transitions), are reported in Table 6. We consider them numerous enough to conclude that SEM-4 with its underlying Hamiltonian works reasonably well only for  $\text{I(a,+)}$ ,  $\text{I(e,+)}$ . For  $\text{I(a,-)}$ ,  $\text{I(e,-)}$  and  $\text{II(a,-)}$ ,  $\text{II(e,-)}$  splittings the disagreement using SEM-4 is complete.

The  $\text{I(a,+)}$ ,  $\text{I(e,+)}$  splittings correspond to a torsional barrier of  $262 \text{ cm}^{-1}$ . 'Related'  $\text{CH}_3\text{NHCl}$  has a torsional barrier of  $1322 \text{ cm}^{-1}$ .<sup>9</sup> Thus, the torsional barrier of  $\text{CH}_3\text{NHCN}$  is closer to the barrier in  $\text{CH}_3-\text{N}=\overset{+}{\text{N}}=\bar{\text{N}}$  ( $250 \text{ cm}^{-1}$ ).<sup>10</sup> The approximate torsional frequency of  $\text{CH}_3\text{NHCN}$  is  $105 \text{ cm}^{-1}$ .

## DISCUSSION

At a slightly higher temperature ( $1000^\circ\text{C}$ )  $(\text{CH}_3)_2\text{NCN}$  also forms  $\text{CH}_2=\text{NCN}$  by pyrolysis.<sup>1</sup> Our present observation of transitions in the interval  $27\,290-29\,137 \text{ MHz}$  (Table 4 of Ref. 1) again raises the question if we may be dealing with spectra of *trans* and/or *cis* iminoacetonitrile (Fig. 4 of Ref. 1) since their estimated (not experimental) rotational constants  $B$  and  $C$  are close to experimental  $B$  and  $C$  for  $\text{CH}_3\text{NHCN}$ . However, iminoacetonitrile is still excluded since neither the *trans* nor the *cis* isomer spectrum will exhibit a,e splitting or inversion phenomena.

As to the structure of  $\text{CH}_3\text{NHCN}$  it was at first expected that the angle  $\alpha$  (Fig. 1) would deviate from  $180^\circ$ . However, assuming  $\alpha = 174^\circ$  with any of the assumed  $\text{N1}-\text{C2}$  or  $\text{C2}\equiv\text{N2}$  distances above seriously damaged the calculated, non-assumed distance ( $\text{C2}\equiv\text{N2}$  and  $\text{N1}-\text{C2}$ , respectively).

*Acknowledgements.* Thanks are due to G. O. Sørensen, N. W. Larsen, and Th. Pedersen of this laboratory for permission to use their computer programs ROTFIT (G.O.S.) and SEM-4. The Danish Research Council for Natural Sciences has supported this work.

## REFERENCES

1. Bak, B., Nielsen, O. J. and Svanholt, H. *Chem. Phys. Lett.* 59 (1978) 330.

2. Wollrab, J. E. and Laurie, V. W. *J. Chem. Phys.* 48 (1968) 5058.
3. Mirri, A. M. and Caminati, W. *J. Mol. Spectrosc.* 47 (1973) 204.
4. Bak, B., Larsen, N. W. and Svanholt, H. *Acta Chem. Scand. A* 31 (1977) 755.
5. Kitawaki, R. and Sugino, K. *J. Org. Chem.* 25 (1960) 1043.
6. Bak, B. and Svanholt, H. *Chem. Phys. Lett.* 66 (1979) 387.
7. Sørensen, G. O. *Available on request.*
8. Larsen, N. W. and Pedersen, T. *Available on request.*
9. Caminati, W., Cervellati, R. and Mirri, A. M. *J. Mol. Spectrosc.* 51 (1974) 288.
10. Salathiel, M. W. and Curl, R. F., Jr. *J. Chem. Phys.* 44 (1966) 1288.
11. Heise, H. M., Lutz, H. and Dreizler, H. Z. *Naturforsch. Teil A* 29 (1974) 1345.

Received July 23, 1979.